



# Rechargeable self-assembled droplet microswimmers driven by surface phase transitions

Diana Cholakova<sup>1</sup>, Maciej Lisicki<sup>2</sup>, Stoyan K. Smoukov<sup>3</sup>, Slavka Tcholakova<sup>1</sup>, E. Emily Lin<sup>3</sup>, Jianxin Chen<sup>3,4</sup>, Gabriele De Canio<sup>5</sup>, Eric Lauga<sup>5</sup> and Nikolai Denkov<sup>1</sup>

**The design of artificial microswimmers is often inspired by the strategies of natural microorganisms. Many of these creatures exploit the fact that elasticity breaks the time-reversal symmetry of motion at low Reynolds numbers, but this principle has been notably absent from model systems of active, self-propelled microswimmers. Here we introduce a class of microswimmers that spontaneously self-assembles and swims without using external forces, driven instead by surface phase transitions induced by temperature variations. The swimmers are made from alkane droplets dispersed in an aqueous surfactant solution, which start to self-propel on cooling, pushed by rapidly growing thin elastic tails. When heated, the same droplets recharge by retracting their tails, swimming for up to tens of minutes in each cycle. Thermal oscillations of approximately 5 °C induce the swimmers to harness heat from the environment and recharge multiple times. We develop a detailed elasto-hydrodynamic model of these processes and highlight the molecular mechanisms involved. The system offers a convenient platform for examining symmetry breaking in the motion of swimmers exploiting flagellar elasticity. The mild conditions and biocompatible media render these microswimmers potential probes for studying biological propulsion and interactions between artificial and biological swimmers.**

Due to their relative simplicity, natural microswimmers<sup>1,2</sup> and their artificial counterparts<sup>3–5</sup> are convenient systems for studying the complex behaviour of active matter. Indeed, intricate nanomachinery governs movement, from cell shaping and division to the propulsion of microorganisms in biology<sup>6</sup>. Developments in molecular machines<sup>3</sup> including nanocars<sup>7</sup> foreshadow such life-like complexity in artificial swimmers, but fabrication and integration from molecular to nano- and microscales is non-trivial: a major challenge is finding robust ways to couple and integrate the energy-consuming building blocks to the mechanical structure<sup>8</sup>. To this end, promising non-biological artificial muscles have already achieved programmable movement<sup>9</sup> and phase-transition-driven two-way elastic deformation<sup>10</sup>. Combinatorial approach methodology to multifunctionality<sup>11</sup> has resulted in self-sensing muscles<sup>12</sup>, and bottom-up synthesis techniques can be used to synthesize single molecules into polymer shapes<sup>13</sup>. A number of mechanisms for artificial swimmers have been used, including prominently chemical power<sup>14</sup>—catalytic particles creating bubbles, self-electrophoresis or releasing slightly dissolving compounds to drive Marangoni flows (for example, camphor boats)<sup>15</sup>. Others are driven by physical effects—thermophoresis<sup>16</sup> or external acoustic<sup>17</sup>, magnetic<sup>18</sup> and electric<sup>19</sup> fields, and they serve as a basis for the theoretical understanding of ‘active matter’<sup>20</sup>.

Three main classes have emerged that are relatively easy to make in large quantities and are therefore accessible for the study of large ensembles of microparticle swarms. The first class—catalytic Janus microswimmers<sup>5</sup>—use catalysts on one side of their surface (for

example, Pt or Pd) to decompose hydrogen peroxide in the surrounding solution, creating micro- or nanobubbles, and self-propel while the chemical fuel lasts.

The second major class of artificial microswimmers<sup>21</sup> uses light-absorbing Janus particles to induce local heating and asymmetric demixing in a binary lutidine/water mixture, thus generating spatial concentration gradients that induce self-diffusiophoretic motion of the particles. Both types of system have been extensively studied, but the need of toxic peroxide or lutidine prevents the study of such swimmers interacting with biological microswimmers in their native environment.

The third class of microswimmers are compatible with biological media and exploit external light or magnetic fields to create motion. Differential light absorption on relatively easy to fabricate Janus particles has been used for thermophoresis. Such swimmers have achieved  $\sim 50 \mu\text{m s}^{-1}$  speeds with hollow particles, which allow loading with drugs for targeted delivery<sup>22</sup>. More recently, emulsion-based Pickering immobilization was employed to scale up and simplify the fabrication of such metal-containing Janus particles, capable of thermophoretic swimming<sup>23</sup>. Their potential beyond drug delivery also extends to therapies such as thrombosis ablation treatment<sup>24</sup>. Magnetic swimmers require more involved microfabrication of intricate screw-type structures<sup>25</sup>, which, however, can be controlled in deep tissues without restrictions for transparency or complications of light absorption. Therefore, they have excellent properties for the studies of mixed artificial and biological swimmers. Magnetic microrobots picked, encapsulated and delivered cells to

<sup>1</sup>Department of Chemical and Pharmaceutical Engineering, Faculty of Chemistry and Pharmacy, Sofia University, Sofia, Bulgaria. <sup>2</sup>Institute of Theoretical Physics, Faculty of Physics, University of Warsaw, Warsaw, Poland. <sup>3</sup>Active and Intelligent Materials Lab, School of Engineering and Materials Science, Queen Mary University of London, London, UK. <sup>4</sup>Department of Applied Chemistry, School of Science, Northwestern Polytechnical University, Xi'an, People's Republic of China. <sup>5</sup>Department of Applied Mathematics and Theoretical Physics, University of Cambridge, Cambridge, UK. ✉e-mail: [maciej.lisicki@fuw.edu.pl](mailto:maciej.lisicki@fuw.edu.pl); [s.smoukov@qmul.ac.uk](mailto:s.smoukov@qmul.ac.uk); [e.lauga@damtp.cam.ac.uk](mailto:e.lauga@damtp.cam.ac.uk); [nd@lcpe.uni-sofia.bg](mailto:nd@lcpe.uni-sofia.bg)

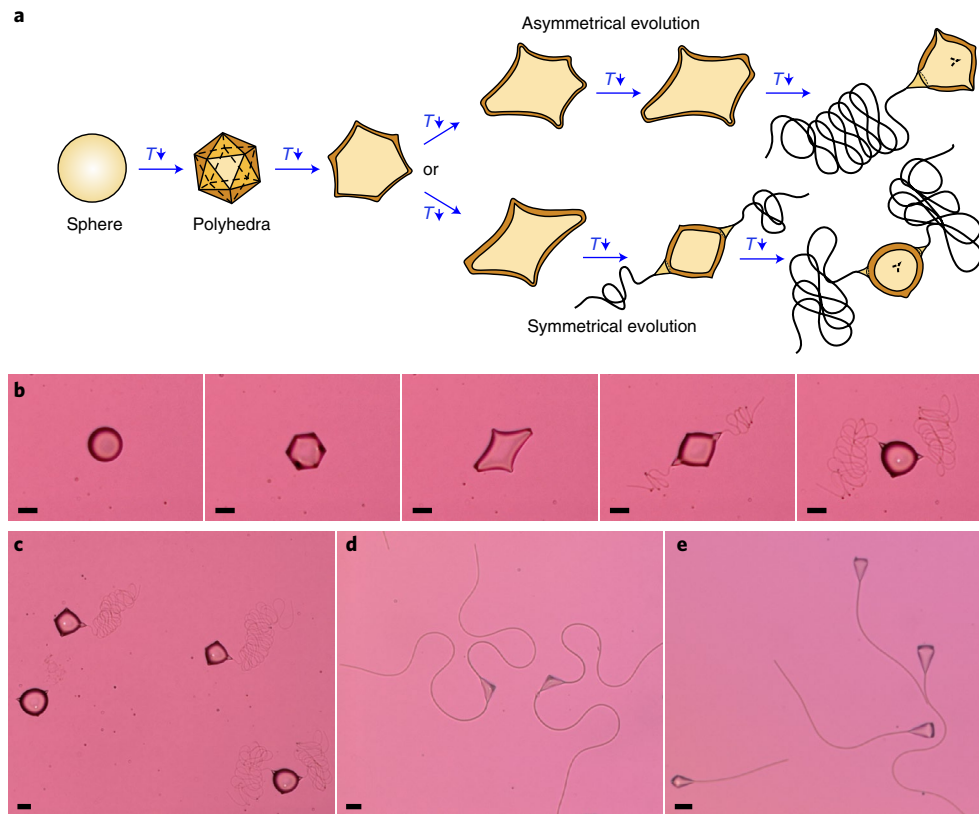


**Fig. 1 | Emulsion droplets deform on cooling and eventually form dynamic swimmers with one or two fibre-extruding nozzles.** **a**, Schematic of the transformation of the initial oil drop into a swimmer with one or two tails, rapidly passing via a series of drop-shape shifts. The  $T \downarrow$  notation above the arrows represents the cooling of the sample. **b**, Images of swimmer formation observed experimentally on cooling a tetradecane drop. **c**, Microscopy image of tetradecane swimmers extruding one or two fibres with a diameter of  $\sim 0.5 \mu\text{m}$ ; extrusion rate  $U_f \approx 6.5 \mu\text{m s}^{-1}$  for drops extruding two fibres and  $U_f \approx 12 \mu\text{m s}^{-1}$  for drops extruding a single fibre. The swimmer speed is  $U_s \approx 0.25 \mu\text{m s}^{-1}$  for drops extruding two fibres and  $U_s \approx 0.50 \mu\text{m s}^{-1}$  for drops extruding a single fibre. **d, e**, Images of pentadecane swimmers extruding fibres with a diameter of  $\sim 2 \mu\text{m}$ . Swimmers extruding two fibres at  $U_f \approx 2.3 \pm 0.3 \mu\text{m s}^{-1}$  and swimmer speed  $U_s \approx 0.45 \pm 0.06 \mu\text{m s}^{-1}$  (**d**) and swimmers extruding one fibre with  $U_f \approx 0.85 \pm 0.10 \mu\text{m s}^{-1}$  and swimmer speed  $U_s \approx 0.28 \pm 0.05 \mu\text{m s}^{-1}$  (**e**). In all experiments, the alkane drops are dispersed in 1.5 wt% Brij 58 surfactant solution. Scale bars, 20  $\mu\text{m}$ . The quoted values of  $U_s$  and  $U_f$  are for the specific drops shown in these images. The relation between  $U_s$  and  $U_f$  is expressed by equation (3). The statistically averaged values of parameter  $c$  in equation (3) are presented and discussed in the main text.

locations while protecting them from shear forces<sup>26</sup>, while others were used to capture non-motile sperm cells, propel them and fertilize an egg<sup>27</sup>. Since external magnetic fields synchronize all the swimmers' movements and orientation, this class possesses some inherent limitations for studying complexity in active matter.

Nonetheless, a minimal non-living model swimmer, which is easy to generate (for example, by self-assembly) and operates in biologically compatible media, remains an outstanding experimental challenge. This challenge is considerably more difficult if one wishes to assemble a swimmer that uses elasticity for hydrodynamic propulsion, can internally store energy and can be recharged.

Here we present a new class of active microswimmers grown via bottom-up molecular self-assembly using only three simple components: alkane oil drops and water containing a dissolved surfactant. The operating temperature window is tuneable by the choice of oil and surfactant, and small ( $\sim 5^\circ\text{C}$ ) thermal oscillations in the environment are sufficient to drive and recharge the swimmers, requiring no additional fuel. The experiment requires only an optical microscope with a thermally controlled sample holder. The compatibility of our system with bacteria and higher organisms<sup>28,29</sup> provides an opportunity to study interactions between artificial and biological swimmers, also in populated swarms.

On cooling, the alkane droplets spontaneously eject thin elastic filaments, which—due to viscous friction with the surrounding

fluid—push the droplets and induce swimming. On subsequent heating of the environment, the filaments retract completely, thus returning the droplets to their initial state and recharging the system. The internal liquid-to-plastic phase transition that occurs on the surface of the oil drops and drives these phenomena is reversible, while the inherent elasticity of the filaments breaks the time-reversal symmetry of the droplet motion (although the latter occurs at low Reynolds numbers), thus generating partially irreversible swimming motion. Developing a detailed elasto-hydrodynamic model of the filament dynamics, we provide a quantitative insight into the swimming behaviour of the droplets and highlight some similarities with the beating patterns of flagellated swimmers<sup>30</sup>.

As an illustration, we present results obtained with oily drops of alkane (pentadecane or tetradecane), placed in  $\sim 1.5$  wt% aqueous surfactant solution (Brij 58) that is cooled at a rate of  $0.1$ – $1.0^\circ\text{C min}^{-1}$ , down to  $\sim 8^\circ\text{C}$  for pentadecane ( $C_{15}$ ) or  $\sim 2^\circ\text{C}$  for tetradecane ( $C_{14}$ ). The cooling results in initial changes in the drop shape, which quickly reach a steady-state spheroidal shape with four (or five) 'spikes' arranged in the positions of the corners of a tetrahedron (or of a pentagonal pyramid with a tetragonal base) at the particle surface (Fig. 1). One or two of the spikes transform into nozzles that quickly extrude material from the sphere into long filaments with a uniform diameter (Fig. 1 and Supplementary Videos 1–3). We observed that swimmers with a single tail are preferably

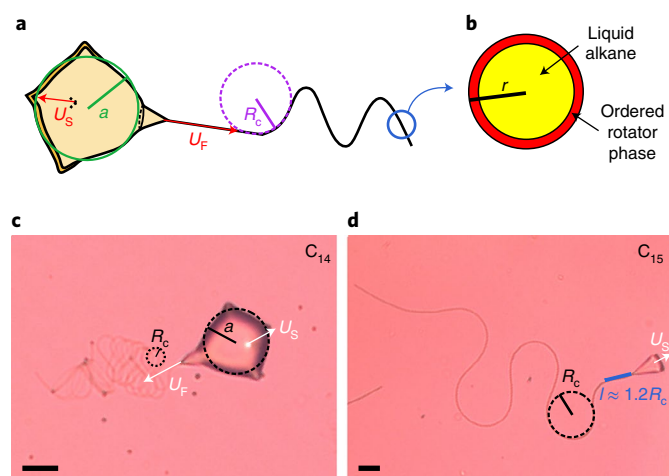


**Fig. 2 | Main parameters describing the swimmers shape and motion. a**, Detailed diagram of the spiked ball swimmer, where the effective swimmer radius is  $a$ ; swimmer velocity,  $U_s$ ; fibre extrusion velocity,  $U_F$ ; and radius of curvature of the first filament bend,  $R_c$ . The filament radius is  $r$  and plastic shell thickness,  $\delta$ . **b**, Schematic cross-section of the fibre. In the centre, the fibres are filled with liquid oil, whereas ordered layers of plastic rotator phase are formed on their surface. This rotator phase ensures the fibres' elasticity. **c,d**, Microscopy images of one-tailed swimmers overlaid with several different quantities measured from the experiment. The swimmer shown in **c** is made from tetradecane oil and that in **d** from pentadecane oil. Scale bars, 20  $\mu\text{m}$ .

formed at lower cooling rates (for example,  $0.1\text{ }^\circ\text{C min}^{-1}$ ), whereas the main fraction of swimmers had two tails at a higher cooling rate ( $\sim 0.5\text{ }^\circ\text{C min}^{-1}$ ), while drops with one and two tails were observed to coexist in the same sample in the transition range of cooling rates, namely,  $\sim 0.2\text{--}0.3\text{ }^\circ\text{C min}^{-1}$ . No notable dependence of the number of extruded tails on the drop size was observed, thus excluding a strong influence of the local interfacial curvature for spikes transformation into fibre-extruding nozzles.

$C_{15}$  and  $C_{14}$  droplets extruded fibres with notably different diameters, namely,  $d \approx 2.0 \pm 0.2\text{ }\mu\text{m}$  for  $C_{15}$  and  $d \approx 0.5 \pm 0.1\text{ }\mu\text{m}$  for  $C_{14}$ , independently of whether one or two fibres were extruded from a given drop (Fig. 1b,c and Fig. 1d,e show illustrative examples, respectively). For convenience, hereafter, we term the fibres for  $C_{15}$  drops as ‘thick’ and for  $C_{14}$  drops as ‘thin’.

The time for which swimming can be observed in a given system mostly depends on the cooling rate. Depending on the specific oil–surfactant combination, the swimmers are observed in a specific temperature range, for example,  $3\text{--}4\text{ }^\circ\text{C}$  wide for  $C_{15}$  drops. Performing experiments with different cooling rates, we change the duration of the period in which the emulsion temperature falls within this range. For example, at a cooling rate of  $0.50\text{ }^\circ\text{C min}^{-1}$ , about  $5\text{--}10\text{ min}$  is available for swimming, whereas this time is  $\sim 20\text{ min}$  at a lower cooling rate of  $0.15\text{ }^\circ\text{C min}^{-1}$ .

In our previous studies, quasi-static shapes were obtained on the slow cooling of emulsion droplets<sup>31</sup>. The experiments showed that these shape transformations (artificial morphogenesis) were driven by the formation of a two-dimensional plastic rotator phase at the drop surface, with somewhat different stability in microconfinement than bulk rotator phases<sup>32</sup>, and with thickness between several and dozens of nanometres, depending on the system<sup>31,33</sup>. This plastic rotator phase is formed at the edges of the deformed drops (that is, at the edges of polyhedral shapes, at the periphery of flattened platelets and on the surface of cylindrical protrusions), thus forming a frame of plastic rods that gradually extends with time by incorporating new alkane molecules from the liquid interior of the drops. The molecules in the rotator phase have some rotational freedom and

occupy a larger volume compared with the truly crystalline phase of the alkanes—this freedom leads to higher molecular mobility and inherent plasticity of the rotator phases. The energy gain on the formation of this plastic rotator phase on the surface of the deforming drops is greater than the energy penalty from the expanding interfacial area, where the interfacial energy was measured to be in the range of  $3\text{ to }10\text{ mJ m}^{-2}$  (ref. <sup>34</sup>). Molecular dynamics tools to model rotator phase transitions were only recently established<sup>35</sup>, but the main stages of the observed drop-shape evolution sequence were explained with a theoretical model that analysed the energy dependence on the droplet shape, which included both drop surface energy and energy of the forming plastic frame<sup>36,37</sup>. The observed shapes were also interpreted and discussed<sup>38</sup> as a new type of ‘tensegrity’ (tensorial integrity) structure<sup>39</sup>, which acquire mechanical stability by balancing the compression stress of the interfacial tension with rigidity of the plastic frame forming at the drop surface.

In the new class of oil–surfactant systems described here, the previously observed transformations occur very quickly and the drops rapidly transmuted into swimmers (Fig. 1 and Supplementary Videos 1–3). As all the other shape changes are driven by a few layers of plastic phase formed on the surface of the self-shaping drops, we postulate that the elastic filaments have a similar structure. Therefore, the swimmers' actuation is caused by self-assembled thin elastic flagella-like tails (Fig. 2a) with a shell of thickness  $\delta$  composed of alkane molecules ordered in a plastic rotator phase and an interior of liquid alkane (Fig. 2b). Our experiments showed that two main conditions should be simultaneously satisfied to observe swimmers of this type: (1) the surfactant should be with a longer tail than alkane molecules so that the adsorption layers of the surfactant freeze before the drop interior; (2) the cooling rate should be very low, around  $\leq 1\text{ }^\circ\text{C}$ , thus allowing the drops to pass through all the preceding stages to form a swimmer before their complete freezing.

We quantify the relationships between all key parameters describing the behaviour of the observed swimmers. The swimming,  $U_s$ , and extrusion,  $U_F$ , speeds were measured to increase approximately linearly with the cooling rate, which is consistent with the faster formation of the plastic phase on the drop surface (Fig. 3a). Both  $U_s$  and  $U_F$  are notably higher for single-tailed swimmers compared with two-tailed swimmers at a given cooling rate. This result is also expected, because the rate of plastic phase formation on the drop surface is expected to be the same for a given system and cooling rate, independent of the number of extruded fibres, while this same phase is distributed into one or two fibres in the two types of swimmer. Under equivalent conditions, droplets with a smaller initial diameter extrude fibres at a lower rate compared with bigger droplets, again because bigger drops have a higher surface area from which the rotator phase of the fibres originates. All these experimental trends are quantitatively captured in the model explained below (equation (3)).

To clarify the origin of this new type of microswimmer propulsion, we balance the hydrodynamic Stokes drag on the rapidly extruding cylindrical filaments with the drag created by the friction of the propelled mother drop (approximated as a sphere) with the surrounding fluid. The resulting elasto-hydrodynamic model of the swimmers advances the understanding of elastic fibre extrusion dynamics<sup>40–42</sup> and is described in detail in Supplementary Section II. Briefly, because of the filaments friction with the viscous medium, we estimate the fibre elastic stiffness from the measured periodicity of fibre buckling with characteristic wavelength  $l$  (Fig. 2). While past calculations only focussed on hydrodynamic friction and bending of fibres with a fixed basis<sup>40</sup>, our theoretical approach builds on a different numerical scheme<sup>41</sup> and fully characterizes free particle swimming using the extrusion of elastic filament (Fig. 2). The relationship that we derive between the swimming speed of a droplet extruding one or two filaments,  $U_s$ , and the extrusion speed of that filament,  $U_F$ , is

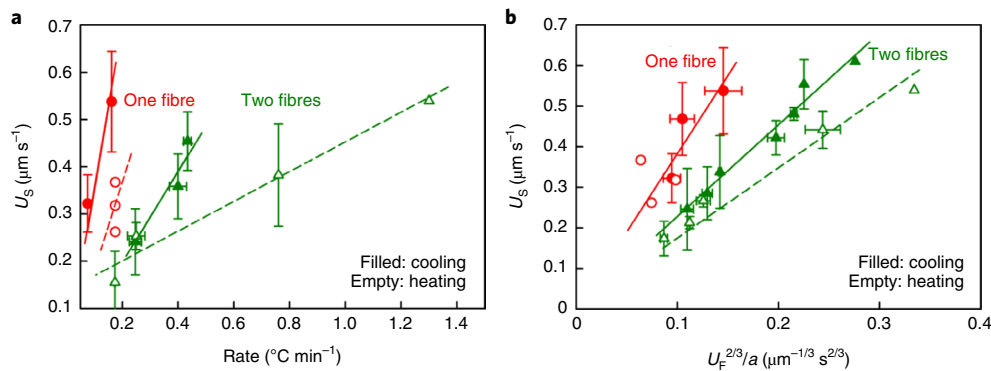


**Fig. 3 | Droplet swimming speed. a**, Dependence of swimming speed,  $U_s$ , on cooling rate (filled symbols) and heating rate (empty symbols) for  $C_{15}$  swimmers in 1.5 wt% Brij 58 solution, extruding one fibre (red circles) or two fibres (green triangles). **b**, Relation between swimming speed,  $U_s$ , fibre extrusion speed,  $U_F$ , and drop radius,  $a$ , for the same experimental data (equation (3)). Note that equation (3) used to construct the plot in **b** is derived only for the extruding fibres—the data with retraction are shown for comparison only. The error bars represent the standard deviations calculated from our data points.

$$U_s = c U_F l/a, \quad (1)$$

where  $a$  is the radius of the main body of the swimmer and  $c$  is a dimensionless constant. We treat the filaments as a uniform in length material with characteristic (elasto-hydrodynamic) buckling length  $l$ , which depends on the bending stiffness  $A$ , extrusion speed and resistance to the flow of filament in the direction parallel to its axis per unit length  $\xi_{\parallel}$  as

$$l = (A/\xi_{\parallel} U_F)^{1/3}. \quad (2)$$

The results of our simulations show that the buckling length can be extracted from the radius of curvature  $R_c$  of the first buckle, which is measured with high precision from the experimental observations, as  $l \approx 1.2R_c$  (Fig. 2). Combining equations (1) and (2) with the theoretical estimates<sup>42</sup> for  $\xi_{\parallel}$ , we are able to describe the dynamics of the swimmer using  $a$ ,  $l$ ,  $U_F$  and  $U_s$  as experimentally accessible quantities, while  $c$  and  $A$  were determined from equations (1) and (2), respectively. We analysed more than 50 swimmers in total, finding the swimming speed  $U_s$  to be rather high, around  $1 \mu\text{m s}^{-1}$ , and appears as 10–50% of  $U_F$  of thick fibres and 3–5% of  $U_F$  of thin fibres. From these experiments, we determined bending stiffness  $A \approx 210 \pm 60 \text{ Nm}^2$  with  $l \approx 25 \pm 5 \mu\text{m}$  for thick fibres and  $A \approx 25 \pm 8 \text{ Nm}^2$  with  $l \approx 7 \pm 2 \mu\text{m}$  for thin fibres. Both one-tailed and two-tailed swimmers are described by this model with the same value of the only material parameter  $A$ , a clear indication of the self-consistency of the theoretical approach. This interpretation also showed that the constant  $c$  is fairly independent of the materials used and the drop size. Statistically averaging the values of  $c$  determined for the individual droplets, we obtained  $c \approx 0.142 \pm 0.035$  for swimmers with one filament, which is  $\sim 50\%$  higher than  $c \approx 0.093 \pm 0.031$  determined for swimmers extruding two filaments in the same system, probably because the propulsion forces exerted by the two fibres in the two-tailed swimmers do not act in the same direction.

The combination of equations (1) and (2) yields the following relationship, which can be experimentally verified:

$$U_s = \frac{c}{a} \left( \frac{A}{\xi_{\parallel}} \right)^{1/3} U_F^{2/3}. \quad (3)$$

Indeed, the plot of  $U_s$  versus  $U_F^{2/3}/a$  for swimmers of the same composition, which presumably have the same values of  $A$  and  $\xi_{\parallel}$ , gives a straight line (Fig. 3b). Note that the scaling prediction in equation (3) reflects the intricate coupling between the hydrodynamic

propulsion force created by the extruding fibre and its elastic properties, which lead to fibre buckling and thus modulating the propulsion force (Supplementary Section IV.G provides further details).

With our model, we also quantitatively describe the undulations of the orientation angle of the swimmers with respect to their direction of motion (Fig. 4). Using the experimentally available values of  $a$ ,  $l$  and  $U_F$ , we predict the period and amplitude of the angle oscillations, which agrees very well with the measured data for the last two quantities (Supplementary Table 2 and Supplementary Sections IV.F and IV.I).

The retraction of fibres—on subsequent emulsion heating—is also of high interest, because it defines the reversibility of the process. The retraction is driven by the positive interfacial tension at the oil–water interface, which draws the fibre inwards to minimize the liquid interfacial area. This is unlike fibre extrusion where buckling instability is coupled with elasticity-induced undulations; during retraction, both fibre and droplet are pulled towards a single point on the nozzle, resulting in reduced undulating movement of the droplet–filament system. The quantitative comparison of the data for fibre extrusion and contraction shows that the swimmer speeds during extrusion are higher than those on retraction at the same magnitudes of cooling and heating rates (Fig. 3a). The slope of the relation between  $U_s$  and  $U_F^{2/3}/a$  is also somewhat lower for retraction in the case of two-tailed swimmers (Fig. 3b). This difference in the swimming speeds on cooling and heating—enabled by fibre elasticity—shows that the swimming is partially reversible. A similar difference is also observed in simulations (Supplementary Videos 4 and 5). Further experiments are needed to more precisely quantify the irreversibility of the observed processes.

The analysis of two-tailed droplets suggests an analogy with biological swimmers. The undulating motion of our swimmers resembles—to some extent—that of several eukaryotic microorganisms that swim by waving their flexible flagella. In particular, the swimmers that extrude two fibres show similarities to the motion exhibited by biflagellate algae, akin to *Chlamydomonas reinhardtii* (Supplementary Videos 2 and 3). One question for these biological swimmers concerns the mechanism by which their two flagella synchronize. It had long been thought that the synchrony of beating flagella is achieved through hydrodynamic interaction<sup>30,43</sup>, as seen in artificially driven colloidal systems<sup>44</sup>. The flow fields around two single-flagellated algae have also been shown to lead to concerted motion provided the distance of flow-mediated interactions was sufficiently small<sup>45</sup>. This view has been questioned with increasing evidence that intracellular coupling must play a mediatory role in the coordination of beating<sup>46,47</sup>. To test

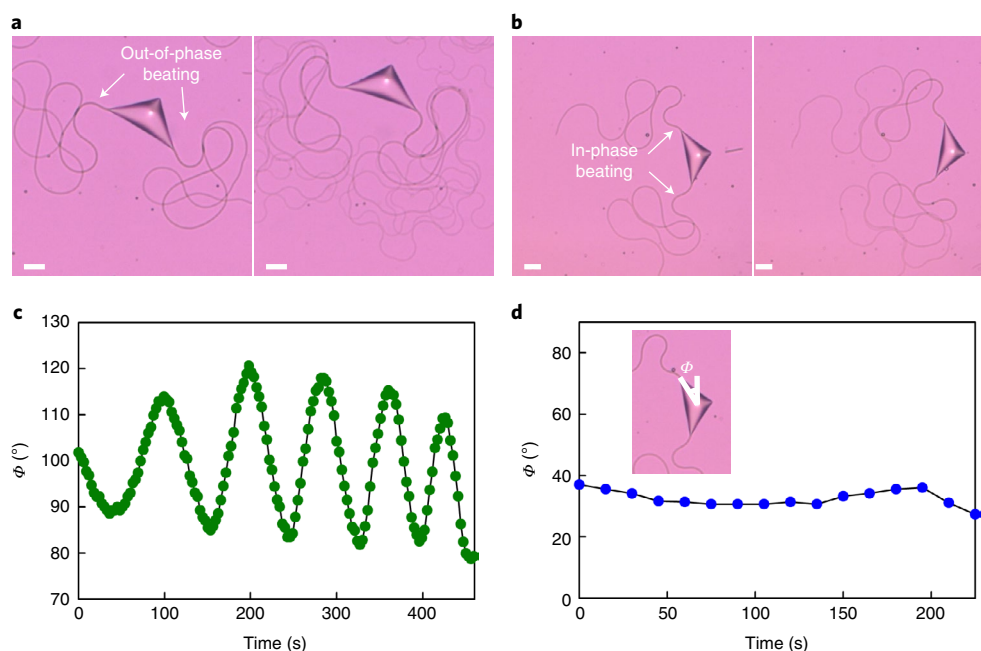


**Fig. 4 | Kinematics of swimming.** **a, b**, Microscopy images of pentadecane swimmers dispersed in 1.5 wt% Brij 58 solution, extruding two fibres. Note that the thickness of the extruded fibres decreases with time due to the molecular rearrangement of the alkane molecules in the fibres and the length of the fibres increases remarkably. The fibres are either extruded out-of-phase (Supplementary Video 3) (**a**) or extruded in-phase (Supplementary Video 2) (**b**). **c, d**, Dependence of angle  $\Phi$  with time. This angle is defined as the angle formed between the extruding tip, the white dot in the centre of the extruding drop and the vertical axis, as shown in the inset in **d**. For out-of-phase extrusion, the angle oscillates with time (**c**), whereas for in-phase extrusion, it remains almost constant (**d**). Scale bars, 20  $\mu\text{m}$ .

these possibilities with our model system, we studied droplets that were extruding two fibres. By analysing the video records, we observed that the extrusion speeds of the two fibres extruded by a given droplet were equal. However, for the various droplets, these pairs of fibres were in different relative phases, which resulted in different ranges of undulation angles  $\Phi$  for the main droplets (Fig. 4 and Supplementary Videos 2 and 3). Unlike the beating patterns observed in *Chlamydomonas* that exhibit changes in the relative phase between the two flagella, our analysis of 30 droplets swimming by extruding two filaments in 12 videos show that for a given droplet, the phase difference between the extruded filaments remains constant without any sign of synchronization. These results suggest that at distances comparable to the sizes of our droplets, the hydrodynamic interactions and coupling through the body of the droplet are too weak to induce a notable change in the phase difference and fibre synchronization. One can expect that the internal coupling inside the organism most likely plays a key role for similarly sized biological swimmers.

Another analogy with living systems is the emergent ability to harvest energy from changes in the environment (for example, in day/night cycles). When we warm rotator phase fibres (often several millimetres long and only a micrometre wide), they fully retract all the way back to the mother drop (Supplementary Videos 6 and 7). Supplying gentle temperature oscillations of less than 5 °C, which do not lead to oil drop freezing, provides enough energy to completely recharge the swimmers in every cooling/heating cycle and let them swim for multiple cycles. Supplementary Video 8 shows a droplet in three consecutive extrusion/retraction cycles. The enthalpy of freezing of hexadecane is  $\Delta H^\circ \approx 235 \text{ kJ kg}^{-1}$  (ref. 48), and since approximately 75% of this enthalpy (that is, 175  $\text{kJ kg}^{-1}$ ) is due to the liquid–rotator phase transition<sup>48</sup>, the stored potential energy in the particles that could be used for swimming exceeds the maximum energy density of a lead–acid battery, namely,  $\sim 140 \text{ kJ kg}^{-1}$  (40  $\text{Wh kg}^{-1}$ ) (ref. 49).

In conclusion, we present a new class of active, elastic microswimmers produced by simply cooling a three-component system—oil droplets in an aqueous surfactant solution. The swimmers in this class are not restricted to the specific examples presented and discussed in this Article. We typically observed such active swimmers when surfactants of different types (ionic or non-ionic) have saturated hydrophobic tails that are one to three carbon atoms longer than the alkane molecules and the emulsions are slowly cooled at  $\sim 0.1\text{--}0.5 \text{ }^\circ\text{C min}^{-1}$ . The temperature interval of the swimming behaviour can be tuned by selecting alkanes with appropriate melting temperature in the drops. Our theoretical model has identified the key parameters governing the motion and may inspire new discoveries in active matter. By coupling buckling instability with filament extrusion, we quantitatively reveal the origin of partial time irreversibility of this mode of swimming at low Reynolds numbers<sup>28</sup> and provide some insights into the motion of living microswimmers. Note that the non-ionic surfactants used in our study are biocompatible and have been applied in various biosystems<sup>50–54</sup>, although the biocompatibility of our systems with real microorganisms has to be investigated in subsequent studies. We highlight the potential for hydrodynamic studies in the area of active matter by referring to mixed systems of artificial and biological microswimmers that can be explored in diluted or in dense populations to reveal collective effects.

### Online content

Any methods, additional references, Nature Research reporting summaries, source data, extended data, supplementary information, acknowledgements, peer review information; details of author contributions and competing interests; and statements of data and code availability are available at <https://doi.org/10.1038/s41567-021-01291-3>.

Received: 11 May 2020; Accepted: 8 June 2021;  
Published online: 15 July 2021

## References

- Elgeti, J., Winkler, R. G. & Gompper, G. Physics of microswimmers—single particle motion and collective behavior: a review. *Rep. Prog. Phys.* **78**, 056601 (2015).
- Lauga, E. & Powers, T. R. The hydrodynamics of swimming microorganisms. *Rep. Prog. Phys.* **72**, 096601 (2009).
- Balzani, V., Credi, A., Raymo, F. M. & Stoddart, J. F. Artificial molecular machines. *Angew. Chem. Int. Ed.* **39**, 3348–3391 (2000).
- Schwarz-Linek, J. et al. Phase separation and rotor self-assembly in active particle suspensions. *Proc. Natl Acad. Sci. USA* **109**, 4052–4057 (2012).
- Paxton, W. F. et al. Catalytic nanomotors: autonomous movement of striped nanorods. *J. Am. Chem. Soc.* **126**, 13424–13431 (2004).
- Michelin, S. & Lauga, E. Efficiency optimization and symmetry-breaking in a model of ciliary locomotion. *Phys. Fluids* **22**, 111901 (2013).
- Kassem, S. et al. Artificial molecular motors. *Chem. Soc. Rev.* **46**, 2592–2621 (2017).
- Fischer, P. Vision statement: interactive materials—drivers of future robotic systems. *Adv. Mater.* **32**, 1–4 (2020).
- Khaldi, A., Elliott, J. A. & Smoukov, S. K. Electro-mechanical actuator with muscle memory. *J. Mater. Chem. C* **2**, 8029–8034 (2014).
- Marshall, J. E., Gallagher, S., Terentjev, E. M. & Smoukov, S. K. Anisotropic colloidal micromuscles from liquid crystal elastomers. *J. Am. Chem. Soc.* **136**, 474–479 (2014).
- Khaldi, A., Plesse, C., Vidal, F. & Smoukov, S. K. Smarter actuator design with complementary and synergetic functions. *Adv. Mater.* **27**, 4418–4422 (2015).
- Wang, T. et al. Electroactive polymers for sensing. *Interface Focus* **6**, 20160026 (2016).
- Lesov, I. et al. Bottom-up synthesis of polymeric micro- and nanoparticles with regular anisotropic shapes. *Macromolecules* **51**, 7456–7462 (2018).
- Sanchez, S., Soler, L. & Katuri, J. Chemically powered micro- and nanomotors. *Angew. Chem. Int. Ed.* **54**, 1414–1444 (2015).
- Soh, S., Bishop, K. J. M. & Grzybowski, B. A. Dynamic self-assembly in ensembles of camphor boats. *J. Phys. Chem. B* **112**, 10848–10853 (2008).
- Jiang, H. R., Yoshinaga, N. & Sano, M. Active motion of a Janus particle by self-thermophoresis in a defocused laser beam. *Phys. Rev. Lett.* **105**, 1–4 (2010).
- Ren, L. et al. 3D steerable, acoustically powered microswimmers for single-particle manipulation. *Sci. Adv.* **5**, eaax3084 (2019).
- Ghosh, A. & Fischer, P. Controlled propulsion of artificial magnetic nanostructured propellers. *Nano Lett.* **9**, 2243–2245 (2009).
- Chang, S. T., Paunov, V. N., Petsev, D. N. & Velev, O. D. Remotely powered self-propelling particles and micropumps based on miniature diodes. *Nat. Mater.* **6**, 235–240 (2007).
- Takatori, S. C. & Brady, J. F. Towards a thermodynamics of active matter. *Phys. Rev. E* **91**, 032117 (2015).
- Buttinoni, I., Volpe, G., Kümmel, F., Volpe, G. & Bechinger, C. Active Brownian motion tunable by light. *J. Phys. Condens. Matter* **24**, 284129 (2012).
- Xuan, M. et al. Near infrared light-powered Janus mesoporous silica nanoparticle motors. *J. Am. Chem. Soc.* **138**, 6492–6497 (2016).
- Lv, H., Xing, Y., Du, X., Xu, T. & Zhang, X. Construction of dendritic Janus nanomotors with H<sub>2</sub>O<sub>2</sub> and NIR light dual-propulsion via a Pickering emulsion. *Soft Matter* **16**, 4961–4968 (2020).
- Shao, J. et al. Erythrocyte membrane modified Janus polymeric motors for thrombus therapy. *ACS Nano* **12**, 4877–4885 (2018).
- Peyer, K. E., Tottori, S., Qiu, F., Zhang, L. & Nelson, B. J. Magnetic helical micromachines. *Chem. Eur. J.* **19**, 28–38 (2013).
- Lee, S. et al. A capsule-type microrobot with pick-and-drop motion for targeted drug and cell delivery. *Adv. Healthcare Mater.* **7**, 1–6 (2018).
- Medina-Sánchez, M., Schwarz, L., Meyer, A. K., Hebenstreit, F. & Schmidt, O. G. Cellular cargo delivery: toward assisted fertilization by sperm-carrying micromotors. *Nano Lett.* **16**, 555–561 (2016).
- Cates, M. E. Diffusive transport without detailed balance in motile bacteria: does microbiology need statistical physics? *Rep. Prog. Phys.* **75**, 042601 (2012).
- Robinson, D. G., Hoppenrath, M., Oberbeck, K., Luykx, P. & Ratajczak, R. Localization of pyrophosphatase and V-ATPase in *Chlamydomonas reinhardtii*. *Bot. Acta* **111**, 108–122 (1998).
- Goldstein, R. E. Green algae as model organisms for biological fluid dynamics. *Annu. Rev. Fluid Mech.* **47**, 343–375 (2015).
- Denkov, N., Tcholakova, S., Lesov, I., Cholakova, D. & Smoukov, S. K. Self-shaping of oil droplets via the formation of intermediate rotator phases upon cooling. *Nature* **528**, 392–395 (2015).
- Cholakova, D. & Denkov, N. Rotator phases in alkane systems: in bulk, surface layers and micro/nano-confinements. *Adv. Colloid Interface Sci.* **269**, 7–42 (2019).
- Cholakova, D., Denkov, N., Tcholakova, S., Lesov, I. & Smoukov, S. K. Control of drop shape transformations in cooled emulsions. *Adv. Colloid Interface Sci.* **235**, 90–107 (2016).
- Denkov, N., Cholakova, D., Tcholakova, S. & Smoukov, S. K. On the mechanism of drop self-shaping in cooled emulsions. *Langmuir* **32**, 7985–7991 (2016).
- Burrows, S. A., Korotkin, I., Smoukov, S. K., Boek, E. & Karabasov, S. Benchmarking of molecular dynamics force fields for solid–liquid and solid–solid phase transitions in alkanes. *J. Phys. Chem. B* **125**, 5145–5159 (2021).
- Haas, P. A., Goldstein, R. E., Smoukov, S. K., Cholakova, D. & Denkov, N. Theory of shape-shifting droplets. *Phys. Rev. Lett.* **118**, 1–5 (2017).
- Haas, P. A., Cholakova, D., Denkov, N., Goldstein, R. E. & Smoukov, S. K. Shape-shifting polyhedral droplets. *Phys. Rev. Res.* **1**, 023017 (2019).
- Gordon, R., Hanczyk, M. M., Denkov, N. D., Tiffany, M. A. & Smoukov, S. K. in *Habitability of the Universe before Earth: Astrobiology: Exploring Life on Earth and Beyond* (eds Gordon, R. & Sharov, A.) 427–490 (Academic Press, 2018).
- Fuller, R. B. & Applewhite, E. J. *Synergetics 2: Further Explorations in the Geometry of Thinking* (MacMillan 1979).
- Gosselin, F. P., Neetzow, P. & Paak, M. Buckling of a beam extruded into highly viscous fluid. *Phys. Rev. E* **90**, 052718 (2014).
- De Canio, G., Lauga, E. & Goldstein, R. E. Spontaneous oscillations of elastic filaments induced by molecular motors. *J. R. Soc. Interface* **14**, 20170491 (2017).
- Ui, T. J., Hussey, R. G. & Roger, R. P. Stokes drag on a cylinder in axial motion. *Phys. Fluids* **27**, 787–795 (1984).
- Gueron, S. & Levit-Gurevich, K. Energetic considerations of ciliary beating and the advantage of metachronal coordination. *Proc. Natl Acad. Sci. USA* **96**, 12240–12245 (1999).
- Kotar, J., Leoni, M., Bassetti, B., Cosentino, M. & Cicuta, P. Hydrodynamic synchronization of colloidal oscillators. *Proc. Natl Acad. Sci. USA* **107**, 7669–7673 (2010).
- Brumley, D. R., Wan, K. Y., Polin, M. & Goldstein, R. E. Flagellar synchronization through direct hydrodynamic interactions. *eLife* **3**, 1–15 (2014).
- Wan, K. Y. & Goldstein, R. E. Coordinated beating of algal flagella is mediated by basal coupling. *Proc. Natl Acad. Sci. USA* **113**, E2784–E2793 (2016).
- Geyer, V. F., Jüllicher, F., Howard, J. & Friedrich, B. M. Cell-body rocking is a dominant mechanism for flagellar synchronization in a swimming alga. *Proc. Natl Acad. Sci. USA* **110**, 18058–18063 (2013).
- Small, D. M. *The Physical Chemistry of Lipids: From Alkanes to Phospholipids* (Plenum Press, 1986).
- May, G. J., Davidson, A. & Monahov, B. Lead batteries for utility energy storage: a review. *J. Energy Storage* **15**, 145–157 (2018).
- Yang, X., Xiang, L., Dong, Y., Cao, Y. & Wang, C. Effect of nonionic surfactant Brij 35 on morphology, cloud point, and pigment stability in *Monascus* extractive fermentation. *J. Sci. Food Agric.* **100**, 4521–4530 (2020).
- Yang, X. et al. Effects of nonionic surfactants on pigment excretion and cell morphology in extractive fermentation of *Monascus* sp. NJ1. *J. Sci. Food Agric.* **100**, 1832–1832 (2020).
- Yang, X. et al. Effects of nonionic surfactants on pigment excretion and cell morphology in extractive fermentation of *Monascus* sp. NJ1. *J. Sci. Food Agric.* **99**, 1233–1239 (2019).
- Tang, J. et al. Solid lipid nanoparticles with TPGS and Brij 78: a co-delivery vehicle of curcumin and piperine for reversing P-glycoprotein-mediated multidrug resistance in vitro. *Oncol. Lett.* **13**, 389–395 (2017).
- Tomasi, R. F.-X., Sart, S., Champetier, T. & Baroud, C. N. Individual control and quantification of 3D spheroids in a high-density microfluidic droplet array. *Cell Rep.* **31**, 107670 (2020).

**Publisher's note** Springer Nature remains neutral with regard to jurisdictional claims in published maps and institutional affiliations.

© The Author(s), under exclusive licence to Springer Nature Limited 2021

## Methods

**Preparation of samples and observations.** For the preparation of microswimmers, we used emulsions prepared with tetradecane or pentadecane oil dispersed in 1.5 wt% Brij 58 aqueous surfactant solution prepared with deionized water (purified by an Elix 3 module (Millipore)). All the chemical substances were obtained from Sigma-Aldrich. The surfactant was used as received and the alkanes (purity, 99%) were purified from surface-active contamination by passing through a glass column filled with Florisil adsorbent.

Emulsions were prepared using laboratory microkit membrane emulsification module from Shirasu Porous Glass Technology, working with tubular glass membranes with an outer diameter of 10 mm and a working area of approximately 3 cm<sup>2</sup>. Membranes with mean pore size of 5 and 10 μm were used.

For optical observations, a sample of the prepared emulsion was placed in a glass capillary with rectangular cross-sections (width, 1 or 2 mm; height, 100 μm; length, 50 mm) and the capillary was placed into a custom-made cooling chamber connected to a cryo-thermostat (Julabo CF30), allowing the precise control of temperature. To ensure the correct measurement of temperature, a calibrated thermocouple probe was inserted in the next orifice and the temperatures were recorded during the experiments. All the observations were made in transmitted cross-polarized white light. Long-focus objectives (×10, ×20 and ×50) were used to observe the drops on sample cooling. An additional λ plate (compensator plate) was placed between the polarizer and analyser, the latter two being oriented at 90° with respect to each other. The λ plate was oriented at 45° with respect to both analyser and polarizer. Under these conditions, the liquid background and fluid objects have a magenta colour. Observations were performed with an Axio Imager M2m microscope (Zeiss). The cooling rates applied were varied between 0.05 and 1.00 °C min<sup>-1</sup> and the heating rate, between 0.1 and 3.0 °C min<sup>-1</sup>.

**Procedure for video analysis.** The obtained microscopy images were analysed using ImageJ software to extract data for  $R$ ,  $R_c$ ,  $U_s$  and  $U_p$ . For measurements of  $U_p$ , the built-in segmented-line command was used and the fibres were manually outlined. The fibre extrusion speed was calculated as the slope of the newly extruded fibre length per unit time (Supplementary Fig. 1). For the measurement of  $U_s$ , the MTrackJ plugin was used, which allows an easy tracking of the data versus time (Supplementary Video 9). Due to the complexity of the system, all the measurements were manually performed.

**Reporting Summary.** Further information on research design is available in the Nature Research Reporting Summary linked to this article.

## Data availability

Source data are provided with this paper. The data that support the findings of this study are available from the corresponding authors upon reasonable request.

## Code availability

The code used in this study is available from the corresponding authors upon reasonable request.

## Acknowledgements

This study was funded by the European Research Council (ERC) EMATTER (no. 280078) and the Engineering and Physical Sciences Research Council Fellowship no. EP/R028915/1 to S.K.S. This project has received funding from the ERC under the European Union's Horizon 2020 research and innovation programme (grant agreement no. 682754 to E.L.). The study received financial support from project no. KP-06-DV-4/2019 with the Bulgarian Ministry of Education and Science, under the National Research Program 'VIHREN' to N.D. The work has been supported by the National Science Center of Poland SONATA grant no. 2018/31/D/ST3/02408 to M.L. The study falls under the umbrella of European network COST CA17120 Chemobrionics. We are grateful to M. Paraskova (Sofia University) for her help with part of the image analysis and for the preparation of some figures.

## Author contributions

D.C. discovered the phenomenon and clarified the experimental conditions under which this new type of swimmer is obtained and can be controlled. D.C., S.T. and N.D. suggested studying the process in more detail. D.C. and S.T. designed the experimental part of the study. S.K.S. designed the part of the study about filament retraction. D.C. performed most of the experiments with respect to fibre extrusion, summarized the obtained results and analysed them (with inputs from S.T., N.D. and S.K.S.), while E.E.L., D.C. and J.C. performed most of experiments for fibre retraction (with input from S.K.S.). E.E.L. clarified the experimental conditions for controlled retraction of the tails. S.K.S. made the first analytical model for swimming by using the estimates of sphere and cylinder drag forces. M.L. and E.L. developed the theoretical description for the extrusion of fibre and motion of droplets. S.K.S., D.C. and M.L. analysed movies and developed insights into relating the dynamic features to the material properties of fibres. M.L. and G.D.C. developed the computer code used in the numerical simulations. S.K.S. and N.D. prepared the initial manuscript draft. D.C. edited the manuscript and prepared the figures and movies. M.L. prepared the theoretical part of the Supporting Information. M.L. and E.L. edited the manuscript. All the authors critically read the manuscript and approved it.

## Competing interests

The authors declare no competing interests.

## Additional information

**Supplementary information** The online version contains supplementary material available at <https://doi.org/10.1038/s41567-021-01291-3>.

**Correspondence and requests for materials** should be addressed to M.L., S.K.S., E.L. or N.D.

**Peer review information** *Nature Physics* thanks Marisol Ripoll and the other, anonymous, reviewer(s) for their contribution to the peer review of this work.

**Reprints and permissions information** is available at [www.nature.com/reprints](http://www.nature.com/reprints).

## Reporting Summary

Nature Research wishes to improve the reproducibility of the work that we publish. This form provides structure for consistency and transparency in reporting. For further information on Nature Research policies, see our [Editorial Policies](#) and the [Editorial Policy Checklist](#).

Please do not complete any field with "not applicable" or n/a. Refer to the help text for what text to use if an item is not relevant to your study. For final submission: please carefully check your responses for accuracy; you will not be able to make changes later.

### Statistics

For all statistical analyses, confirm that the following items are present in the figure legend, table legend, main text, or Methods section.

n/a Confirmed

- The exact sample size ( $n$ ) for each experimental group/condition, given as a discrete number and unit of measurement
- A statement on whether measurements were taken from distinct samples or whether the same sample was measured repeatedly
- The statistical test(s) used AND whether they are one- or two-sided  
*Only common tests should be described solely by name; describe more complex techniques in the Methods section.*
- A description of all covariates tested
- A description of any assumptions or corrections, such as tests of normality and adjustment for multiple comparisons
- A full description of the statistical parameters including central tendency (e.g. means) or other basic estimates (e.g. regression coefficient) AND variation (e.g. standard deviation) or associated estimates of uncertainty (e.g. confidence intervals)
- For null hypothesis testing, the test statistic (e.g.  $F$ ,  $t$ ,  $r$ ) with confidence intervals, effect sizes, degrees of freedom and  $P$  value noted  
*Give  $P$  values as exact values whenever suitable.*
- For Bayesian analysis, information on the choice of priors and Markov chain Monte Carlo settings
- For hierarchical and complex designs, identification of the appropriate level for tests and full reporting of outcomes
- Estimates of effect sizes (e.g. Cohen's  $d$ , Pearson's  $r$ ), indicating how they were calculated

*Our web collection on [statistics for biologists](#) contains articles on many of the points above.*

### Software and code

Policy information about [availability of computer code](#)

Data collection *The obtained microscopy pictures were analysed using ImageJ software to extract data for R, Rc, US and UF. For measurement of the swimming speed, US, MTrackJ plugin was used*

Data analysis *Provide a description of all commercial, open source and custom code used to analyse the data in this study, specifying the version used OR state that no software was used.*

For manuscripts utilizing custom algorithms or software that are central to the research but not yet described in published literature, software must be made available to editors and reviewers. We strongly encourage code deposition in a community repository (e.g. GitHub). See the Nature Research [guidelines for submitting code & software](#) for further information.

### Data

Policy information about [availability of data](#)

All manuscripts must include a [data availability statement](#). This statement should provide the following information, where applicable:

- Accession codes, unique identifiers, or web links for publicly available datasets
- A list of figures that have associated raw data
- A description of any restrictions on data availability

*The data that support the findings of this study are available from the corresponding authors upon reasonable request.  
The code used in this study is available from the corresponding authors upon reasonable request.*

## Field-specific reporting

Please select the one below that is the best fit for your research. If you are not sure, read the appropriate sections before making your selection.

Life sciences     Behavioural & social sciences     Ecological, evolutionary & environmental sciences

For a reference copy of the document with all sections, see [nature.com/documents/nr-reporting-summary-flat.pdf](https://www.nature.com/documents/nr-reporting-summary-flat.pdf)

## Life sciences study design

All studies must disclose on these points even when the disclosure is negative.

Sample size	<i>We analyze more than 50 swimmers</i>
Data exclusions	<i>No data exclusion</i>
Replication	<i>30 replications</i>
Randomization	<i>We allocate them by the size of the drops and number of extruded fibers</i>
Blinding	<i>No applicable for this study</i>

## Behavioural & social sciences study design

All studies must disclose on these points even when the disclosure is negative.

Study description	<i>Briefly describe the study type including whether data are quantitative, qualitative, or mixed-methods (e.g. qualitative cross-sectional, quantitative experimental, mixed-methods case study).</i>
Research sample	<i>State the research sample (e.g. Harvard university undergraduates, villagers in rural India) and provide relevant demographic information (e.g. age, sex) and indicate whether the sample is representative. Provide a rationale for the study sample chosen. For studies involving existing datasets, please describe the dataset and source.</i>
Sampling strategy	<i>Describe the sampling procedure (e.g. random, snowball, stratified, convenience). Describe the statistical methods that were used to predetermine sample size OR if no sample-size calculation was performed, describe how sample sizes were chosen and provide a rationale for why these sample sizes are sufficient. For qualitative data, please indicate whether data saturation was considered, and what criteria were used to decide that no further sampling was needed.</i>
Data collection	<i>Provide details about the data collection procedure, including the instruments or devices used to record the data (e.g. pen and paper, computer, eye tracker, video or audio equipment) whether anyone was present besides the participant(s) and the researcher, and whether the researcher was blind to experimental condition and/or the study hypothesis during data collection.</i>
Timing	<i>Indicate the start and stop dates of data collection. If there is a gap between collection periods, state the dates for each sample cohort.</i>
Data exclusions	<i>If no data were excluded from the analyses, state so OR if data were excluded, provide the exact number of exclusions and the rationale behind them, indicating whether exclusion criteria were pre-established.</i>
Non-participation	<i>State how many participants dropped out/declined participation and the reason(s) given OR provide response rate OR state that no participants dropped out/declined participation.</i>
Randomization	<i>If participants were not allocated into experimental groups, state so OR describe how participants were allocated to groups, and if allocation was not random, describe how covariates were controlled.</i>

## Ecological, evolutionary & environmental sciences study design

All studies must disclose on these points even when the disclosure is negative.

Study description	<i>Briefly describe the study. For quantitative data include treatment factors and interactions, design structure (e.g. factorial, nested, hierarchical), nature and number of experimental units and replicates.</i>
Research sample	<i>Describe the research sample (e.g. a group of tagged <i>Passer domesticus</i>, all <i>Stenocereus thurberi</i> within Organ Pipe Cactus National</i>

**Research sample** *Monument), and provide a rationale for the sample choice. When relevant, describe the organism taxa, source, sex, age range and any manipulations. State what population the sample is meant to represent when applicable. For studies involving existing datasets, describe the data and its source.*

**Sampling strategy** *Note the sampling procedure. Describe the statistical methods that were used to predetermine sample size OR if no sample-size calculation was performed, describe how sample sizes were chosen and provide a rationale for why these sample sizes are sufficient.*

**Data collection** *Describe the data collection procedure, including who recorded the data and how.*

**Timing and spatial scale** *Indicate the start and stop dates of data collection, noting the frequency and periodicity of sampling and providing a rationale for these choices. If there is a gap between collection periods, state the dates for each sample cohort. Specify the spatial scale from which the data are taken*

**Data exclusions** *If no data were excluded from the analyses, state so OR if data were excluded, describe the exclusions and the rationale behind them, indicating whether exclusion criteria were pre-established.*

**Reproducibility** *Describe the measures taken to verify the reproducibility of experimental findings. For each experiment, note whether any attempts to repeat the experiment failed OR state that all attempts to repeat the experiment were successful.*

**Randomization** *Describe how samples/organisms/participants were allocated into groups. If allocation was not random, describe how covariates were controlled. If this is not relevant to your study, explain why.*

**Blinding** *Describe the extent of blinding used during data acquisition and analysis. If blinding was not possible, describe why OR explain why blinding was not relevant to your study.*

Did the study involve field work?  Yes  No

## Field work, collection and transport

**Field conditions** *Describe the study conditions for field work, providing relevant parameters (e.g. temperature, rainfall).*

**Location** *State the location of the sampling or experiment, providing relevant parameters (e.g. latitude and longitude, elevation, water depth).*

**Access & import/export** *Describe the efforts you have made to access habitats and to collect and import/export your samples in a responsible manner and in compliance with local, national and international laws, noting any permits that were obtained (give the name of the issuing authority, the date of issue, and any identifying information).*

**Disturbance** *Describe any disturbance caused by the study and how it was minimized.*

## Reporting for specific materials, systems and methods

We require information from authors about some types of materials, experimental systems and methods used in many studies. Here, indicate whether each material, system or method listed is relevant to your study. If you are not sure if a list item applies to your research, read the appropriate section before selecting a response.

### Materials & experimental systems

n/a	Involvement
<input checked="" type="checkbox"/>	<input type="checkbox"/> Antibodies
<input checked="" type="checkbox"/>	<input type="checkbox"/> Eukaryotic cell lines
<input checked="" type="checkbox"/>	<input type="checkbox"/> Palaeontology and archaeology
<input checked="" type="checkbox"/>	<input type="checkbox"/> Animals and other organisms
<input checked="" type="checkbox"/>	<input type="checkbox"/> Human research participants
<input checked="" type="checkbox"/>	<input type="checkbox"/> Clinical data
<input checked="" type="checkbox"/>	<input type="checkbox"/> Dual use research of concern

### Methods

n/a	Involvement
<input checked="" type="checkbox"/>	<input type="checkbox"/> ChIP-seq
<input checked="" type="checkbox"/>	<input type="checkbox"/> Flow cytometry
<input checked="" type="checkbox"/>	<input type="checkbox"/> MRI-based neuroimaging

## Antibodies

**Antibodies used** *Describe all antibodies used in the study; as applicable, provide supplier name, catalog number, clone name, and lot number.*

**Validation** *Describe the validation of each primary antibody for the species and application, noting any validation statements on the manufacturer's website, relevant citations, antibody profiles in online databases, or data provided in the manuscript.*

## Eukaryotic cell lines

Policy information about [cell lines](#)

**Cell line source(s)** *State the source of each cell line used.*

Authentication	<i>Describe the authentication procedures for each cell line used OR declare that none of the cell lines used were authenticated.</i>
Mycoplasma contamination	<i>Confirm that all cell lines tested negative for mycoplasma contamination OR describe the results of the testing for mycoplasma contamination OR declare that the cell lines were not tested for mycoplasma contamination.</i>
Commonly misidentified lines (See <a href="#">ICLAC</a> register)	<i>Name any commonly misidentified cell lines used in the study and provide a rationale for their use.</i>

## Palaeontology and Archaeology

Specimen provenance	<i>Provide provenance information for specimens and describe permits that were obtained for the work (including the name of the issuing authority, the date of issue, and any identifying information).</i>
Specimen deposition	<i>Indicate where the specimens have been deposited to permit free access by other researchers.</i>
Dating methods	<i>If new dates are provided, describe how they were obtained (e.g. collection, storage, sample pretreatment and measurement), where they were obtained (i.e. lab name), the calibration program and the protocol for quality assurance OR state that no new dates are provided.</i>
<input type="checkbox"/> Tick this box to confirm that the raw and calibrated dates are available in the paper or in Supplementary Information.	
Ethics oversight	<i>Identify the organization(s) that approved or provided guidance on the study protocol, OR state that no ethical approval or guidance was required and explain why not.</i>

Note that full information on the approval of the study protocol must also be provided in the manuscript.

## Animals and other organisms

Policy information about [studies involving animals](#); [ARRIVE guidelines](#) recommended for reporting animal research

Laboratory animals	<i>For laboratory animals, report species, strain, sex and age OR state that the study did not involve laboratory animals.</i>
Wild animals	<i>Provide details on animals observed in or captured in the field; report species, sex and age where possible. Describe how animals were caught and transported and what happened to captive animals after the study (if killed, explain why and describe method; if released, say where and when) OR state that the study did not involve wild animals.</i>
Field-collected samples	<i>For laboratory work with field-collected samples, describe all relevant parameters such as housing, maintenance, temperature, photoperiod and end-of-experiment protocol OR state that the study did not involve samples collected from the field.</i>
Ethics oversight	<i>Identify the organization(s) that approved or provided guidance on the study protocol, OR state that no ethical approval or guidance was required and explain why not.</i>

Note that full information on the approval of the study protocol must also be provided in the manuscript.

## Human research participants

Policy information about [studies involving human research participants](#)

Population characteristics	<i>Describe the covariate-relevant population characteristics of the human research participants (e.g. age, gender, genotypic information, past and current diagnosis and treatment categories). If you filled out the behavioural &amp; social sciences study design questions and have nothing to add here, write "See above."</i>
Recruitment	<i>Describe how participants were recruited. Outline any potential self-selection bias or other biases that may be present and how these are likely to impact results.</i>
Ethics oversight	<i>Identify the organization(s) that approved the study protocol.</i>

Note that full information on the approval of the study protocol must also be provided in the manuscript.

## Clinical data

Policy information about [clinical studies](#)

All manuscripts should comply with the ICMJE [guidelines for publication of clinical research](#) and a completed [CONSORT checklist](#) must be included with all submissions.

Clinical trial registration	<i>Provide the trial registration number from <a href="#">ClinicalTrials.gov</a> or an equivalent agency.</i>
Study protocol	<i>Note where the full trial protocol can be accessed OR if not available, explain why.</i>
Data collection	<i>Describe the settings and locales of data collection, noting the time periods of recruitment and data collection.</i>
Outcomes	<i>Describe how you pre-defined primary and secondary outcome measures and how you assessed these measures.</i>

## Dual use research of concern

Policy information about [dual use research of concern](#)

### Hazards

Could the accidental, deliberate or reckless misuse of agents or technologies generated in the work, or the application of information presented in the manuscript, pose a threat to:

- | No                                  | Yes   |
|-------------------------------------|---|
| <input checked="" type="checkbox"/> | <input type="checkbox"/> Public health              |
| <input checked="" type="checkbox"/> | <input type="checkbox"/> National security          |
| <input checked="" type="checkbox"/> | <input type="checkbox"/> Crops and/or livestock     |
| <input checked="" type="checkbox"/> | <input type="checkbox"/> Ecosystems                 |
| <input checked="" type="checkbox"/> | <input type="checkbox"/> Any other significant area |

Other impacts

Hazards

For examples of agents subject to oversight, see the United States Government [Policy for Institutional Oversight of Life Sciences Dual Use Research of Concern](#).

### Experiments of concern

Does the work involve any of these experiments of concern:

- | No                                  | Yes  |
|-------------------------------------|--|
| <input checked="" type="checkbox"/> | <input type="checkbox"/> Demonstrate how to render a vaccine ineffective                             |
| <input checked="" type="checkbox"/> | <input type="checkbox"/> Confer resistance to therapeutically useful antibiotics or antiviral agents |
| <input checked="" type="checkbox"/> | <input type="checkbox"/> Enhance the virulence of a pathogen or render a nonpathogen virulent        |
| <input checked="" type="checkbox"/> | <input type="checkbox"/> Increase transmissibility of a pathogen                                     |
| <input checked="" type="checkbox"/> | <input type="checkbox"/> Alter the host range of a pathogen  |
| <input checked="" type="checkbox"/> | <input type="checkbox"/> Enable evasion of diagnostic/detection modalities                           |
| <input checked="" type="checkbox"/> | <input type="checkbox"/> Enable the weaponization of a biological agent or toxin                     |
| <input checked="" type="checkbox"/> | <input type="checkbox"/> Any other potentially harmful combination of experiments and agents         |

Other combinations

### Precautions and benefits

Biosecurity precautions

Biosecurity oversight

Benefits

Communication benefits

## ChIP-seq

### Data deposition

- Confirm that both raw and final processed data have been deposited in a public database such as [GEO](#).
- Confirm that you have deposited or provided access to graph files (e.g. BED files) for the called peaks.

Data access links

Files in database submission

Genome browser session  
(e.g. [UCSC](#))

Provide a link to an anonymized genome browser session for "Initial submission" and "Revised version" documents only, to enable peer review. Write "no longer applicable" for "Final submission" documents.

## Methodology

Replicates

Describe the experimental replicates, specifying number, type and replicate agreement.

Sequencing depth

Describe the sequencing depth for each experiment, providing the total number of reads, uniquely mapped reads, length of reads and whether they were paired- or single-end.

Antibodies

Describe the antibodies used for the ChIP-seq experiments; as applicable, provide supplier name, catalog number, clone name, and lot number.

Peak calling parameters

Specify the command line program and parameters used for read mapping and peak calling, including the ChIP, control and index files used.

Data quality

Describe the methods used to ensure data quality in full detail, including how many peaks are at FDR 5% and above 5-fold enrichment.

Software

Describe the software used to collect and analyze the ChIP-seq data. For custom code that has been deposited into a community repository, provide accession details.

## Flow Cytometry

### Plots

Confirm that:

- The axis labels state the marker and fluorochrome used (e.g. CD4-FITC).
- The axis scales are clearly visible. Include numbers along axes only for bottom left plot of group (a 'group' is an analysis of identical markers).
- All plots are contour plots with outliers or pseudocolor plots.
- A numerical value for number of cells or percentage (with statistics) is provided.

### Methodology

Sample preparation

Describe the sample preparation, detailing the biological source of the cells and any tissue processing steps used.

Instrument

Identify the instrument used for data collection, specifying make and model number.

Software

Describe the software used to collect and analyze the flow cytometry data. For custom code that has been deposited into a community repository, provide accession details.

Cell population abundance

Describe the abundance of the relevant cell populations within post-sort fractions, providing details on the purity of the samples and how it was determined.

Gating strategy

Describe the gating strategy used for all relevant experiments, specifying the preliminary FSC/SSC gates of the starting cell population, indicating where boundaries between "positive" and "negative" staining cell populations are defined.

- Tick this box to confirm that a figure exemplifying the gating strategy is provided in the Supplementary Information.

## Magnetic resonance imaging

### Experimental design

Design type

Indicate task or resting state; event-related or block design.

Design specifications

Specify the number of blocks, trials or experimental units per session and/or subject, and specify the length of each trial or block (if trials are blocked) and interval between trials.

Behavioral performance measures

State number and/or type of variables recorded (e.g. correct button press, response time) and what statistics were used to establish that the subjects were performing the task as expected (e.g. mean, range, and/or standard deviation across subjects).

## Acquisition

Imaging type(s)

Field strength

Sequence & imaging parameters

Area of acquisition

Diffusion MRI  Used  Not used

Parameters

## Preprocessing

Preprocessing software

Normalization

Normalization template

Noise and artifact removal

Volume censoring

## Statistical modeling & inference

Model type and settings

Effect(s) tested

Specify type of analysis:  Whole brain  ROI-based  Both

Anatomical location(s)

Statistic type for inference (See [Eklund et al. 2016](#))

Correction

## Models & analysis

n/a | Involved in the study

Functional and/or effective connectivity

Graph analysis

Multivariate modeling or predictive analysis

Functional and/or effective connectivity

Graph analysis

Multivariate modeling and predictive analysis